Stationary Josephson current between ***d***-wave superconductors with charge density waves: angular dependences and violations of the corresponding-states relationship

Alexander Gabovich, Alexander Voitenko

(*Kiev, Ukraine*)

Mai Suan Li, H. Szymczak (*Warsaw, Poland*)

Experiment: Angular distribution of gaps and pseudogaps in cuprates

$Bi_{2-y}Pb_ySr_{2-z}La_zCuO_{6+\delta}$

$Bi_2Sr_2CaCu_2O_{8+\delta}$

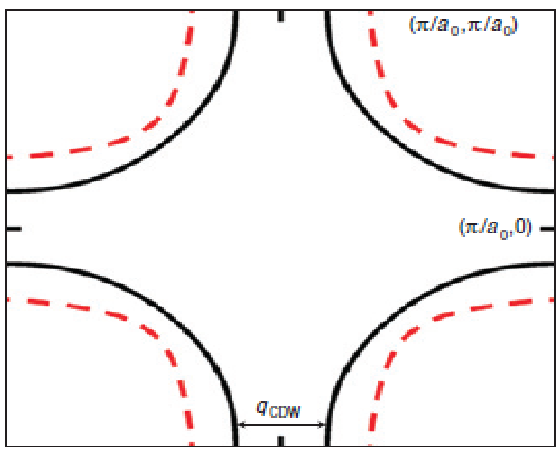

Figure 4 Fermi surface nesting. Tight-binding-calculated Fermi surface (solid black curve) of optimally doped Bi-2201 (ref. 23) based on ARPES data[33]. The nesting wave vector (black arrow) in the antinodal flat band region has length $2\pi/6.2a_0$. Underdoped Bi-2201 Fermi surfaces (shown schematically as red dashed lines) show a reduced volume and longer nesting wave vector, consistent with a CDW origin of the doping-dependent checkerboard pattern reported here.

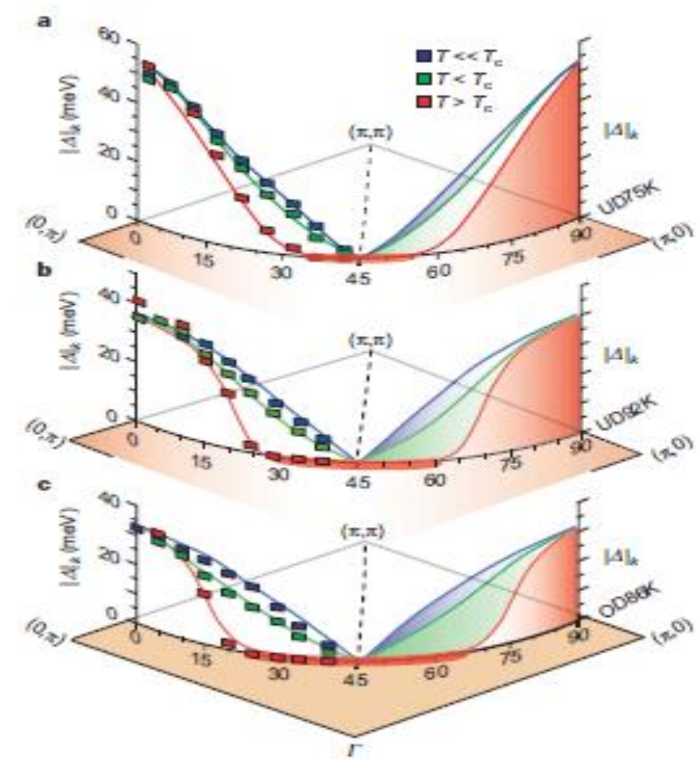

Evidence for charge-density waves (CDWs) in cuprates

$Ca_{2-x}Na_xCuO_2Cl_2$

(STM)

Checkerboard

Bi-based ceramics (STM)

one-dimensional modulation

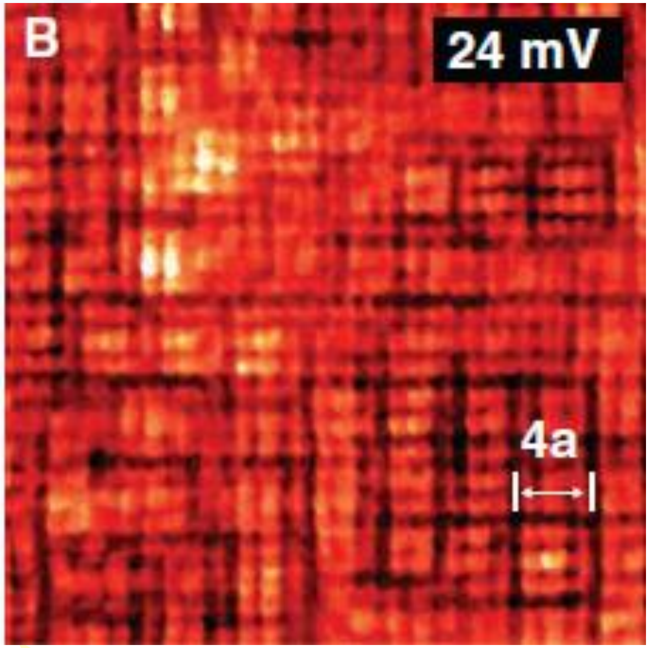

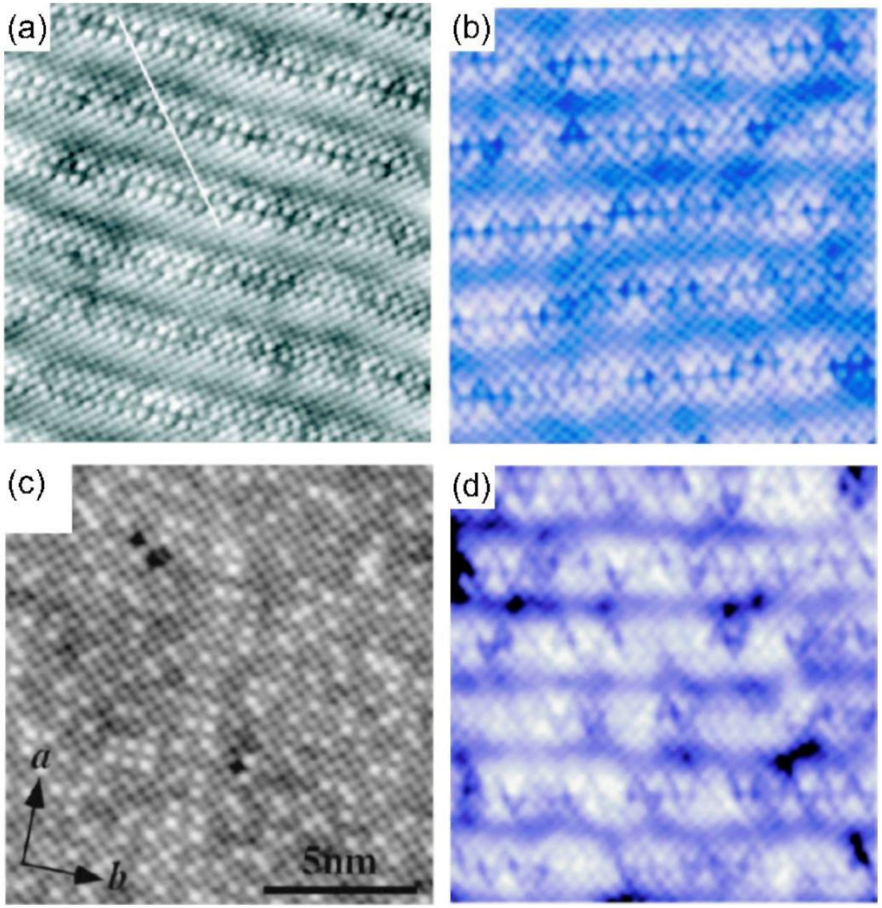

Inherent nanoscale inhomogeneity of measured energy gaps and local critical temperatures ($Bi_2Sr_2CaCu_2O_{8+\delta}$)

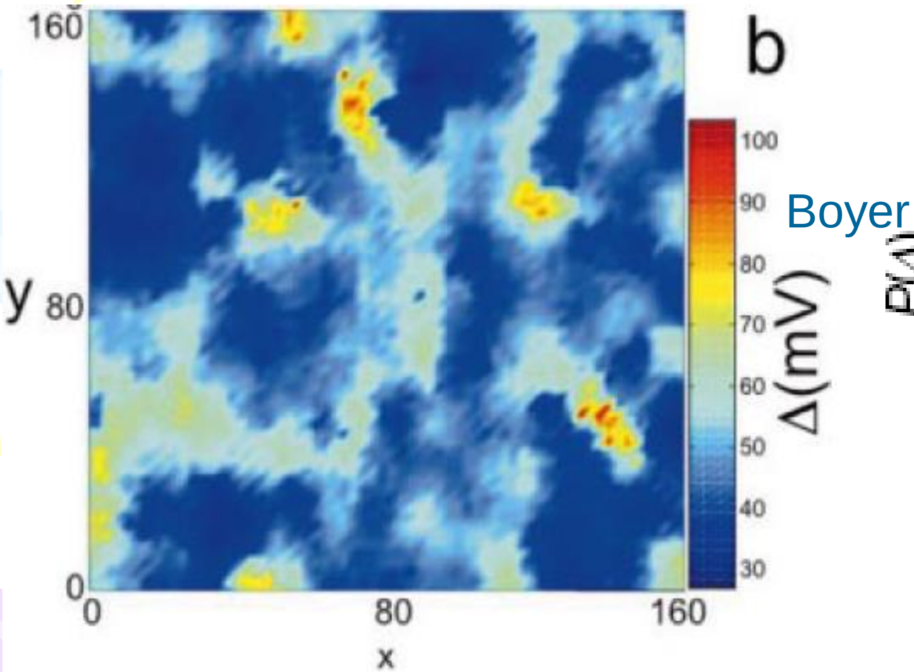

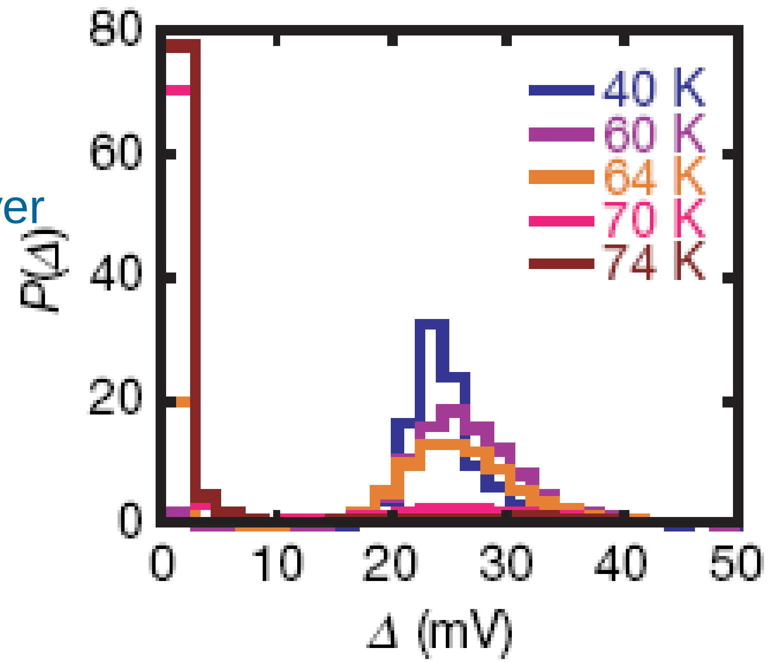

Superconducting gaps are homogeneous, CDW gaps (pseudogaps) vary strongly: Boyer et al. (2007)

FERMI SURFACE MAPS OF THE DIELECTRIC Σ AND SUPERCONDUCTING Δ ORDER PARAMETERS

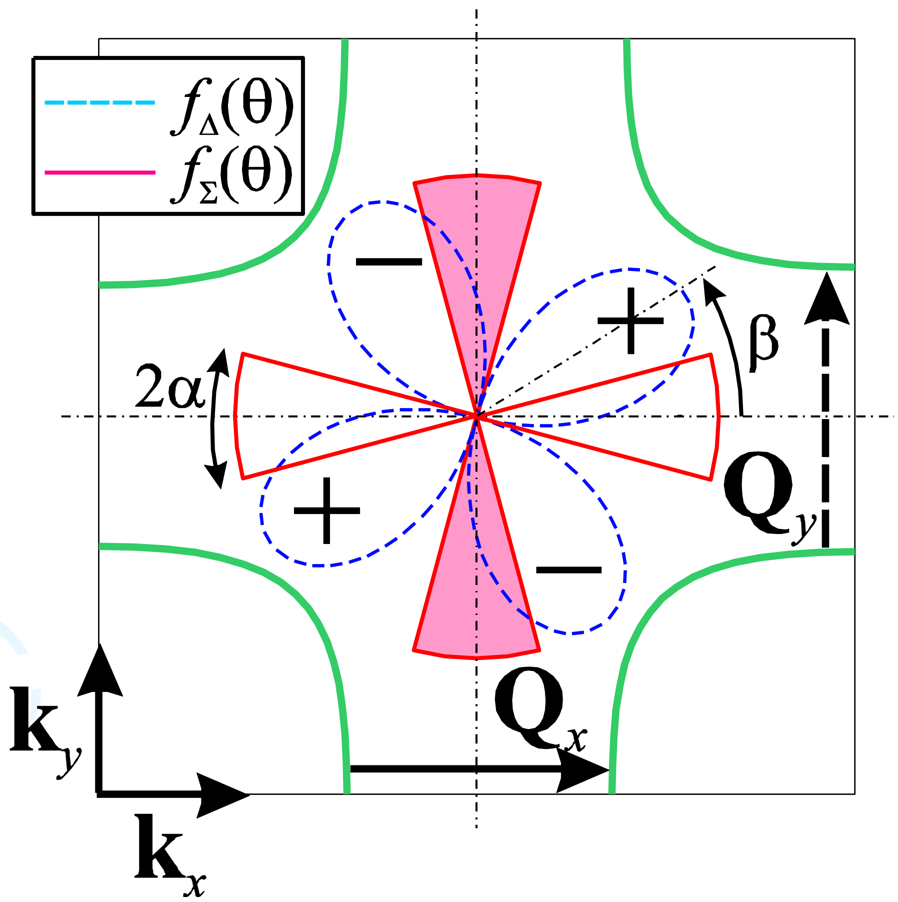

S- and *d*- conventional superconducting pairing

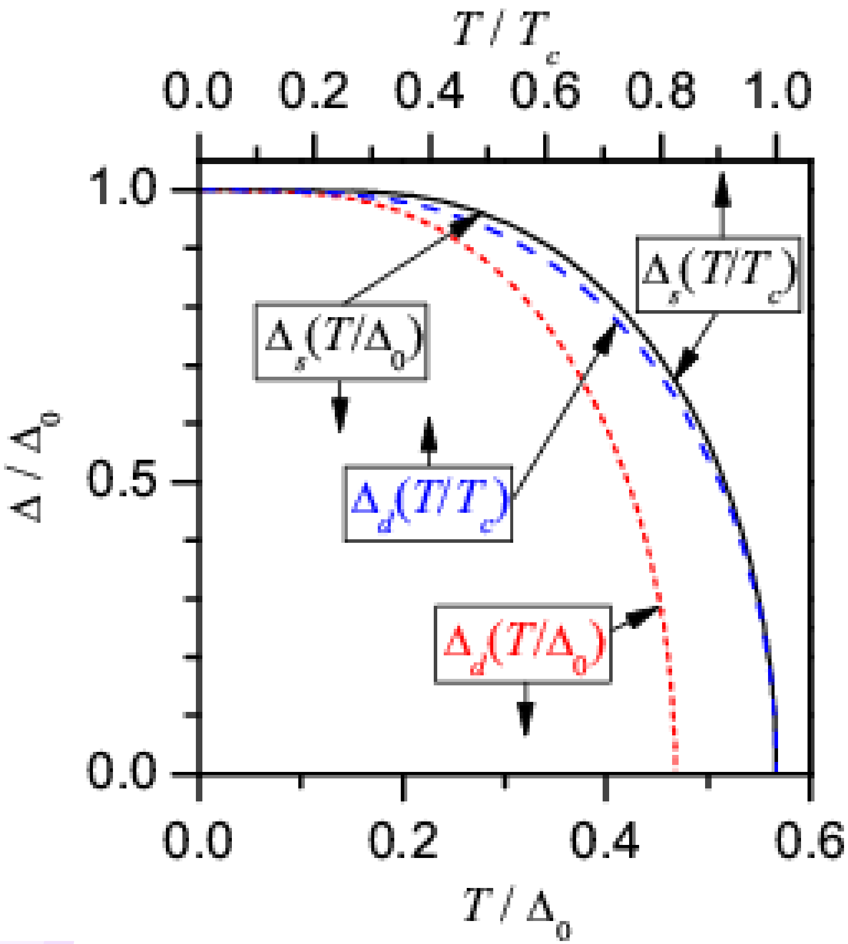

S

$$\frac{\Delta_0}{T_c} \approx 1.76$$

$$\frac{T_c}{\Delta_0} \approx 0.57$$

D

$$\frac{\Delta_0}{T_c} \approx 2.12$$

$$\frac{T_c}{\Delta_0} \approx 0.47$$

THEORETICAL DESCRIPTION

System of equations for order parameters

$$\int_{\beta-\alpha}^{\beta+\alpha} I_M(\sqrt{\Sigma^2 + \Delta^2 \cos^2 2\theta}, k_B T, \Sigma_0) d\theta = 0$$

$$\int_{\beta-\alpha}^{\beta+\alpha} I_M(\sqrt{\Sigma^2 + \Delta^2 \cos^2 2\theta}, k_B T, \Delta_0 \cos 2\theta) \cos^2 2\theta d\theta$$

$$+ \int_{\beta+\alpha}^{\Omega+\beta-\alpha} I_M(\Delta \cos 2\theta, k_B T, \Delta_0 \cos 2\theta) \cos^2 2\theta d\theta = 0$$

In the adopted order parameter configuration

$\mu\Omega = 2\alpha$;

$\Omega = \pi/2$ and π for the checkerboard and unidirectional CDW patterns, respectively; μ = is the dielectrically gapped portion of Fermi surface

Mühlschlegel integral:

$$I_M(X, T, X_0) = \int_0^\infty d\xi \left(\frac{1}{\sqrt{\xi^2 + X^2}} \tanh \frac{\sqrt{\xi^2 + X^2}}{2T} - \frac{1}{\sqrt{\xi^2 + X_0^2}} \right)$$

Δ_0 and Σ_0 are the bare superconducting and CDW order parameters, respectively

$\sigma_0 = \Sigma_0 / \Delta_0$

Phase diagrams

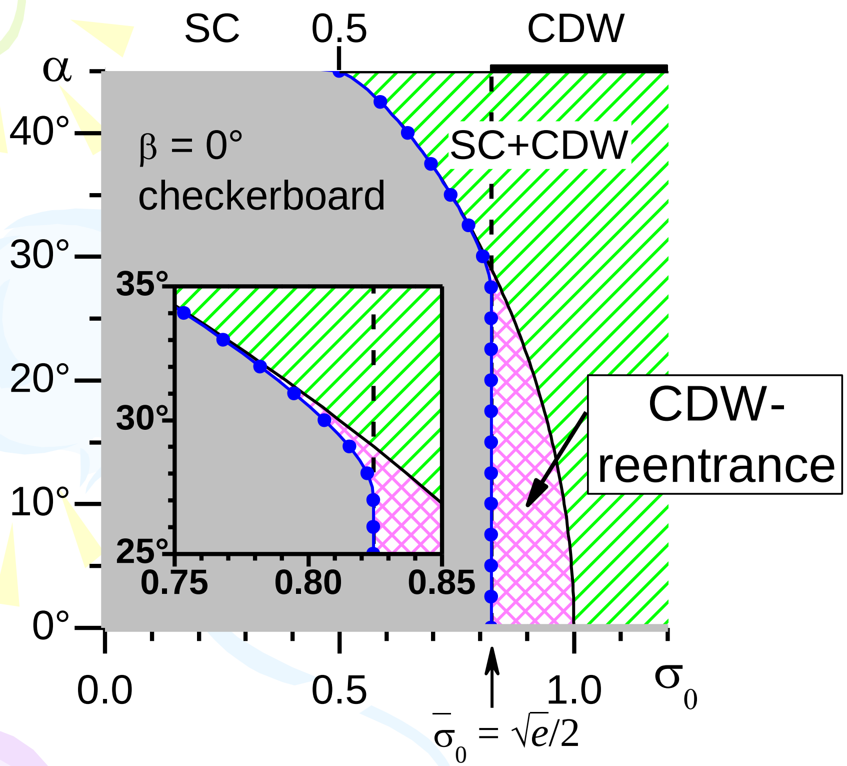

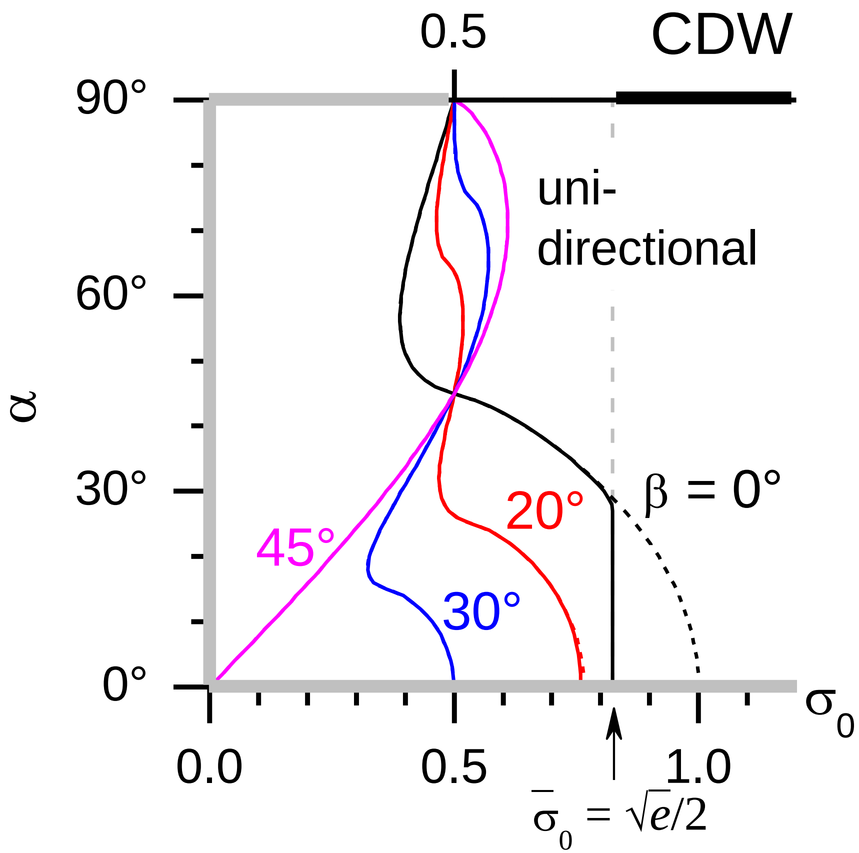

Order parameters

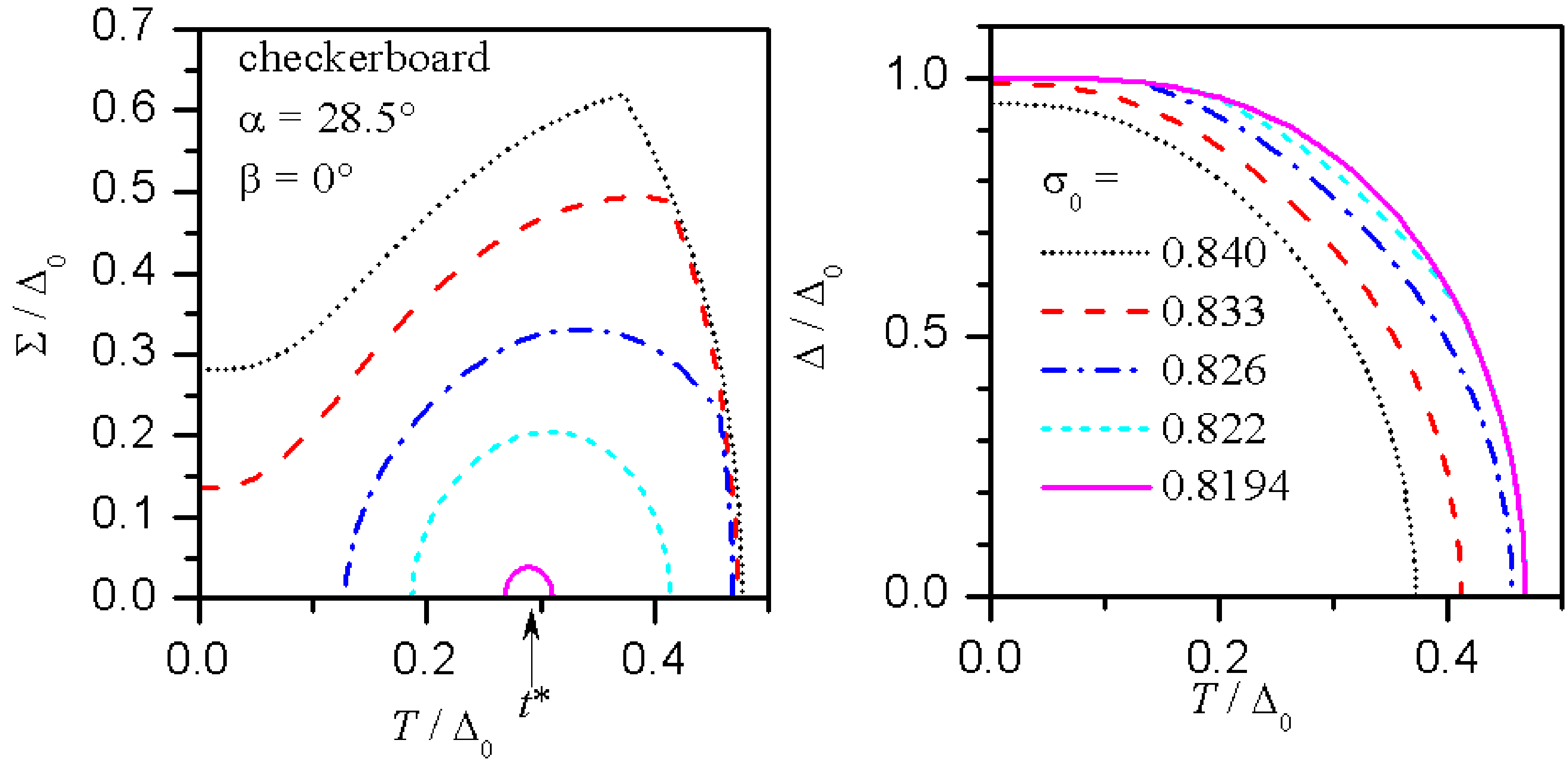

Gap roses

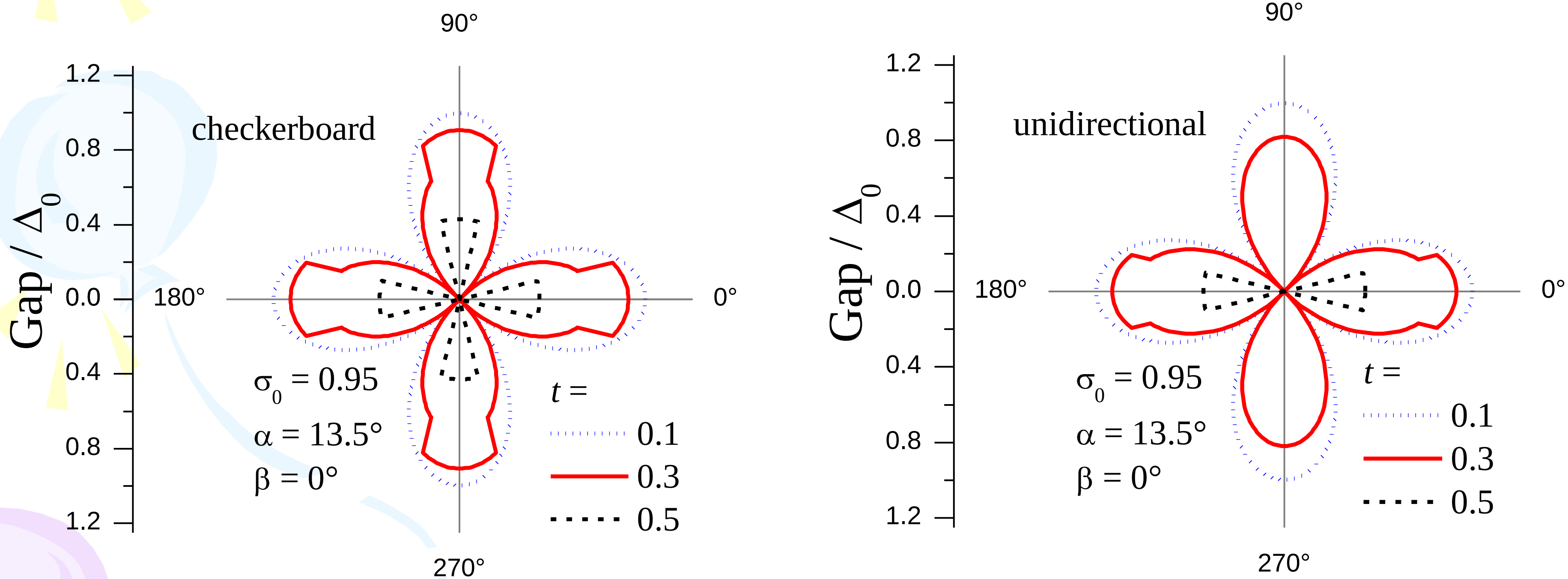
90°
1.2
0.8
0.4
0.0
0.4
0.8
1.2
Gap / Δ0
checkerboard
180°
0°
270°
σ0 = 0.95
α = 13.5°
β = 0°
t =
0.1
0.3
0.5
90°
1.2
0.8
0.4
0.0
0.4
0.8
1.2
Gap / Δ0
unidirectional
180°
0°
270°
σ0 = 0.95
α = 13.5°
β = 0°
t =
0.1
0.3
0.5

dc Josephson current. Geometry of the junction

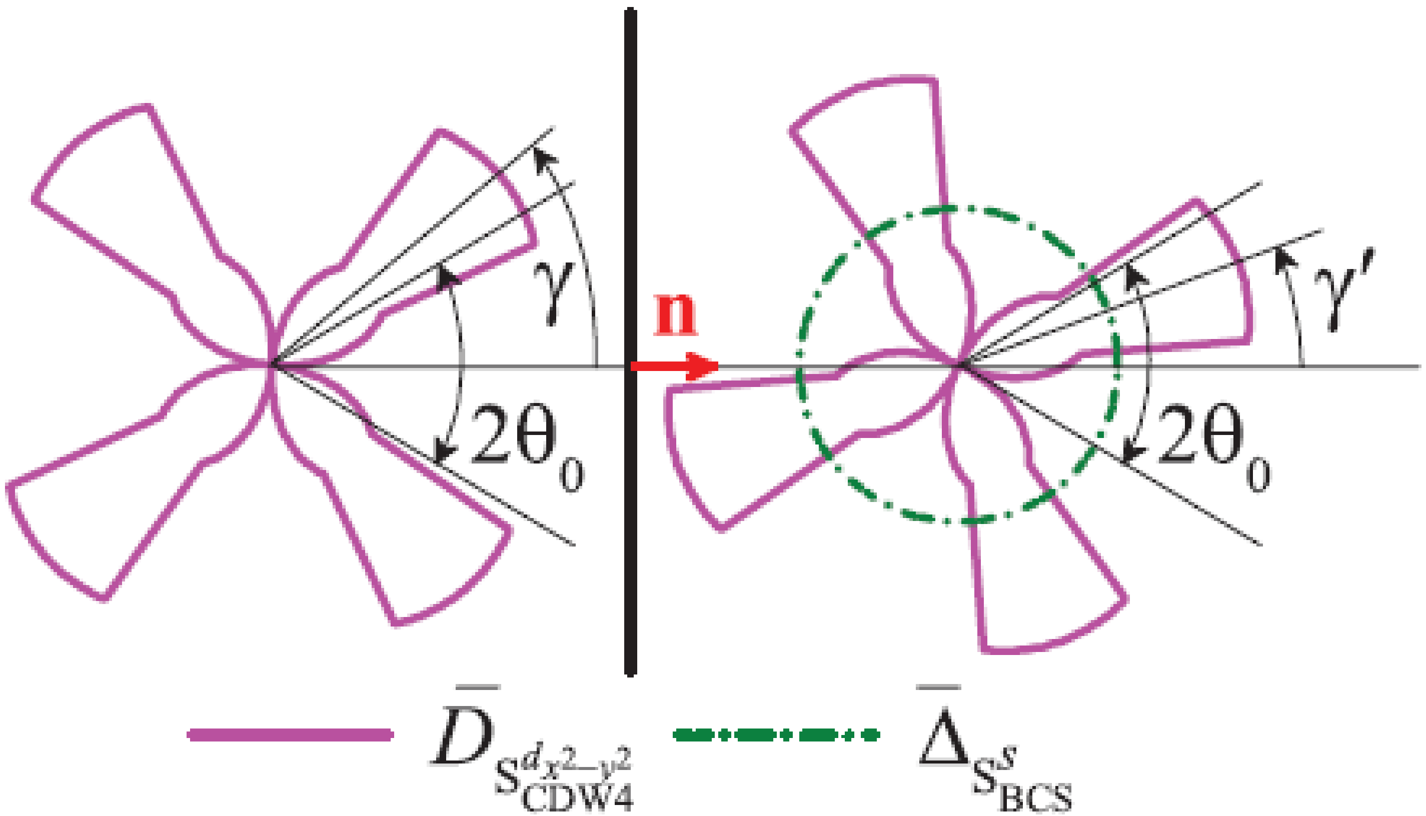

Directional tunneling for an example of non-symmetric junctions

The weight factor $w(\theta)$

$$w(\theta) = \exp\left[-\ln 2 \times \left(\frac{\tan\theta}{\tan\theta_0}\right)^2\right]$$

$$I_c(T) = \frac{\Delta(0)\Delta^*(0)}{2eR_N} i_c(T),$$

$$i_c(T) = \frac{1}{2\pi}\int_{\theta_d} w(\theta)\cos[2(\theta-\gamma)]\, P\left[\Delta^*(T), \sqrt{\Sigma^2 + \Delta^2(T)\cos^2[2(\theta-\gamma)]}\right] d\theta$$

$$+ \frac{1}{2\pi}\int_{\theta_{nd}} w(\theta)\cos[2(\theta-\gamma)]\, P[\Delta^*(T), |\Delta(T)\cos 2(\theta-\gamma)|]\, d\theta.$$

$$P(\Delta_1, \Delta_2) = \int_{\min\{\Delta_1,\Delta_2\}}^{\max\{\Delta_1,\Delta_2\}} \frac{dx \tanh\frac{x}{2T}}{\sqrt{(x^2-\Delta_1^2)(\Delta_2^2-x^2)}}.$$

Parameter dependences of current amplitudes

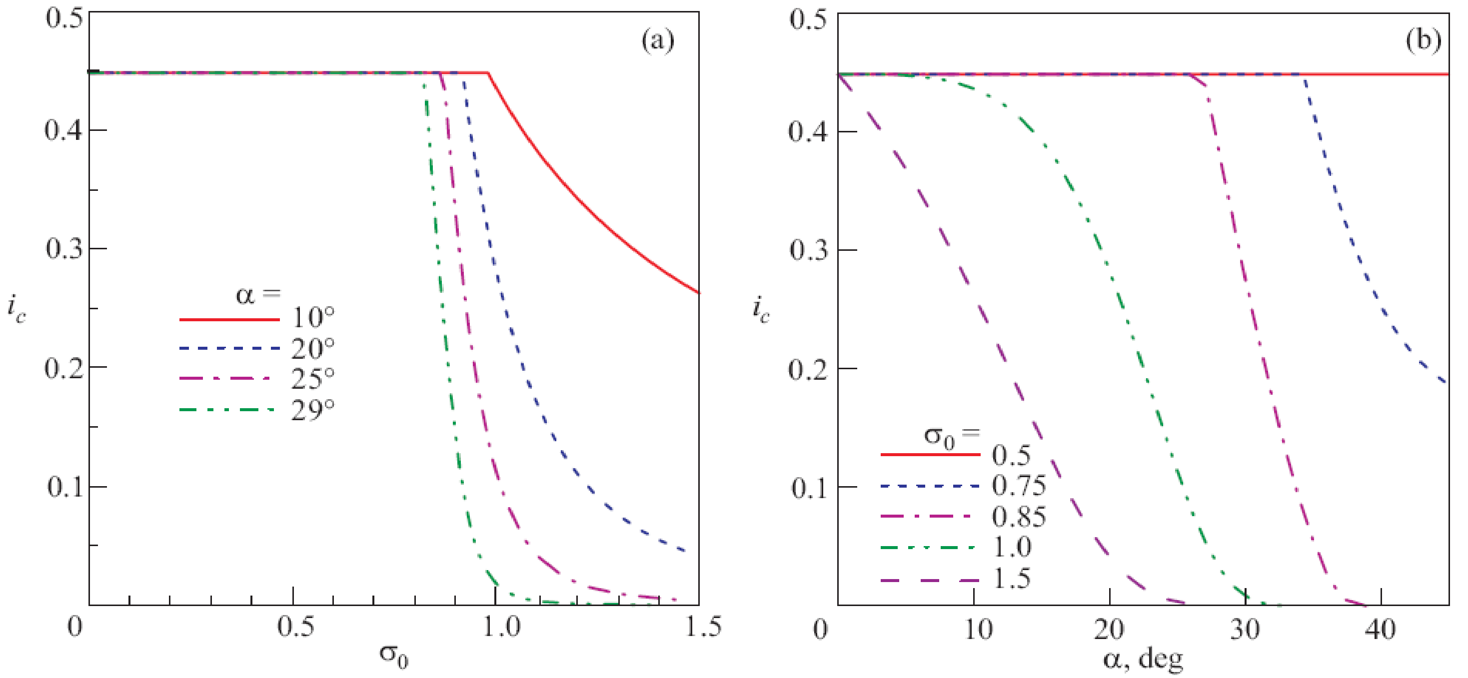

$$S_{CDW4}^{d_{x^2-y^2}} - I - S_{CDW4}^{d_{x^2-y^2}} \text{ junction with } \gamma = \gamma' = 0$$

Parameter dependences of current amplitudes

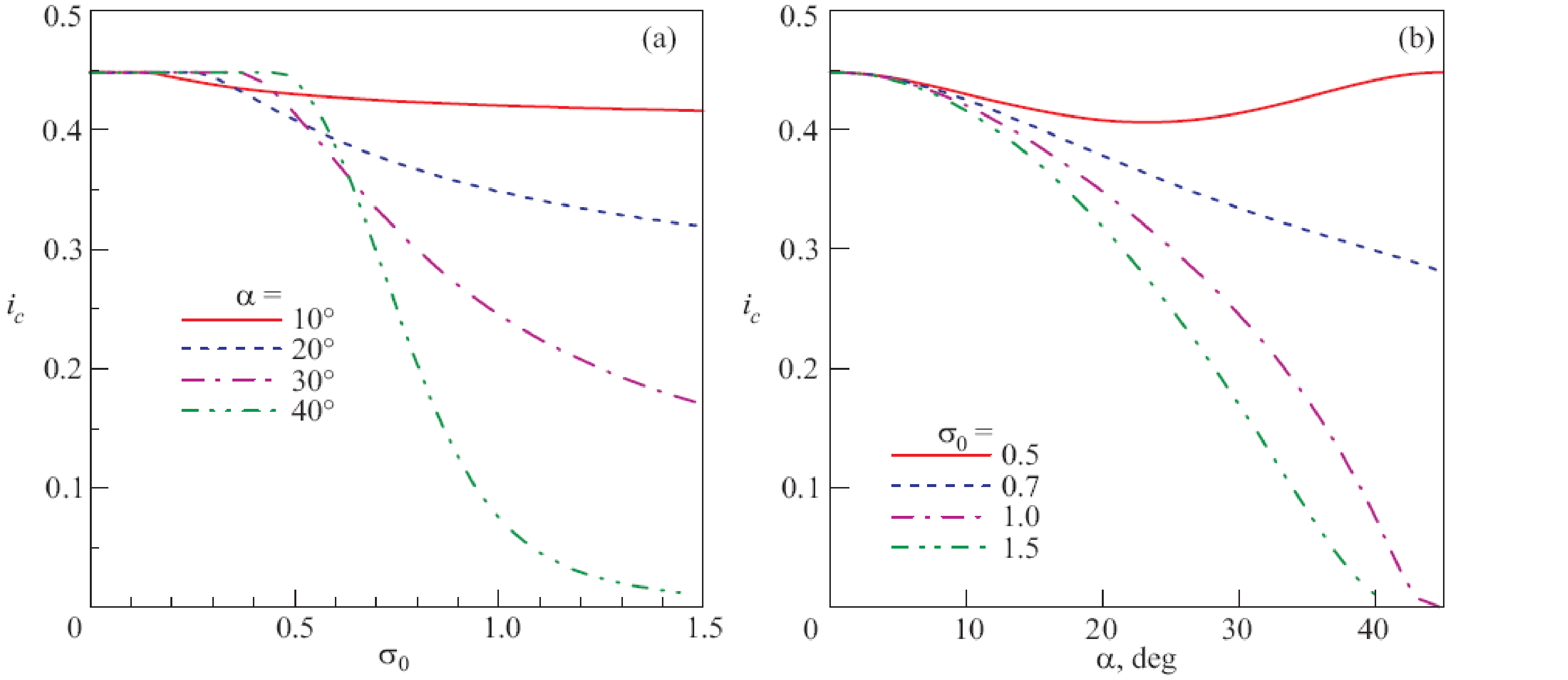

symmetrical $S_{CDW4}^{d_{xy}} - I - S_{CDW4}^{d_{xy}}$ junction

Parameter dependences of current amplitudes

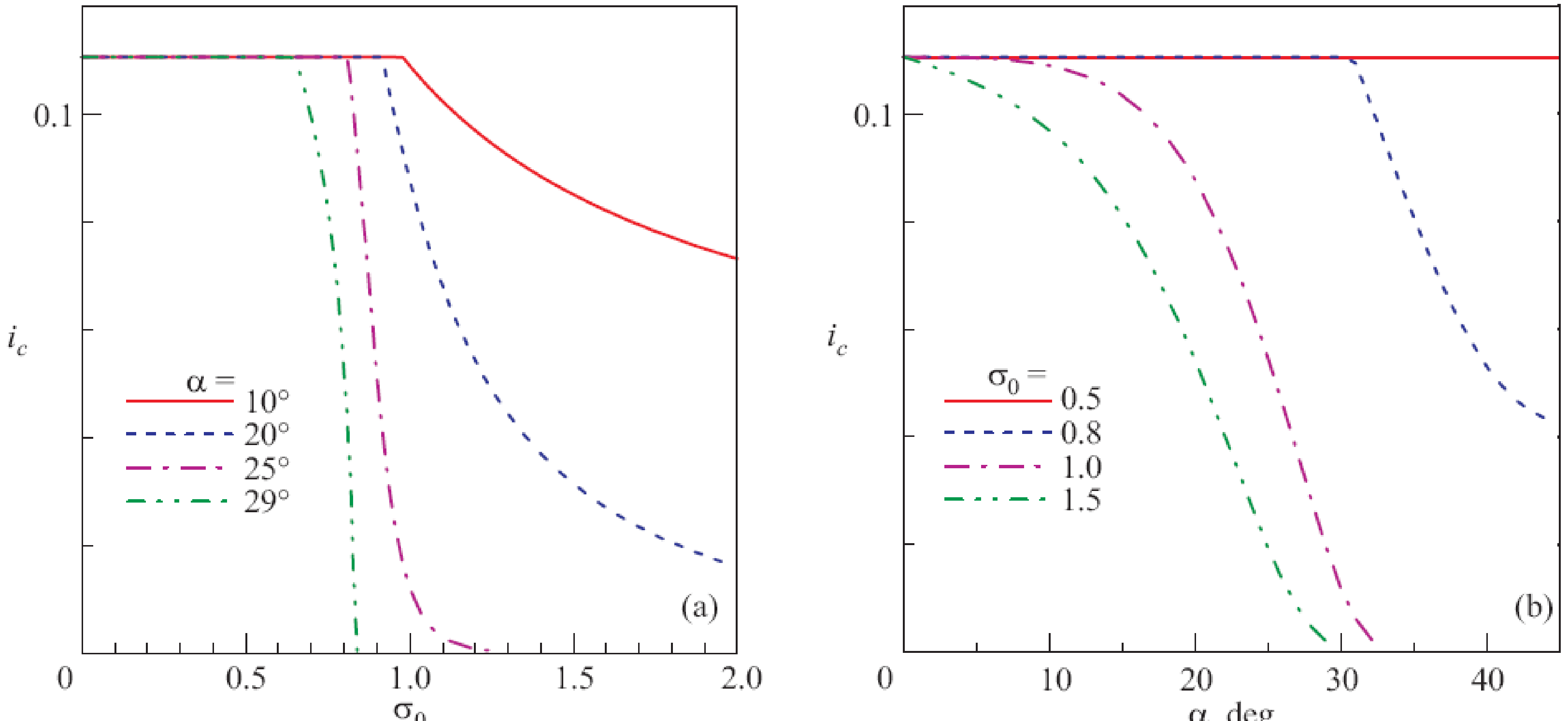

nonsymmetrical $S_{CDW4}^{d_{x^2-y^2}} - I - S_{BCS}^{s}$ junction.

$\delta_{BCS} = 0.1$

$\delta_{BCS} = \Delta_{BCS}(T = 0)/\Delta_0$

Parameter dependences of current amplitudes in the reentrance region

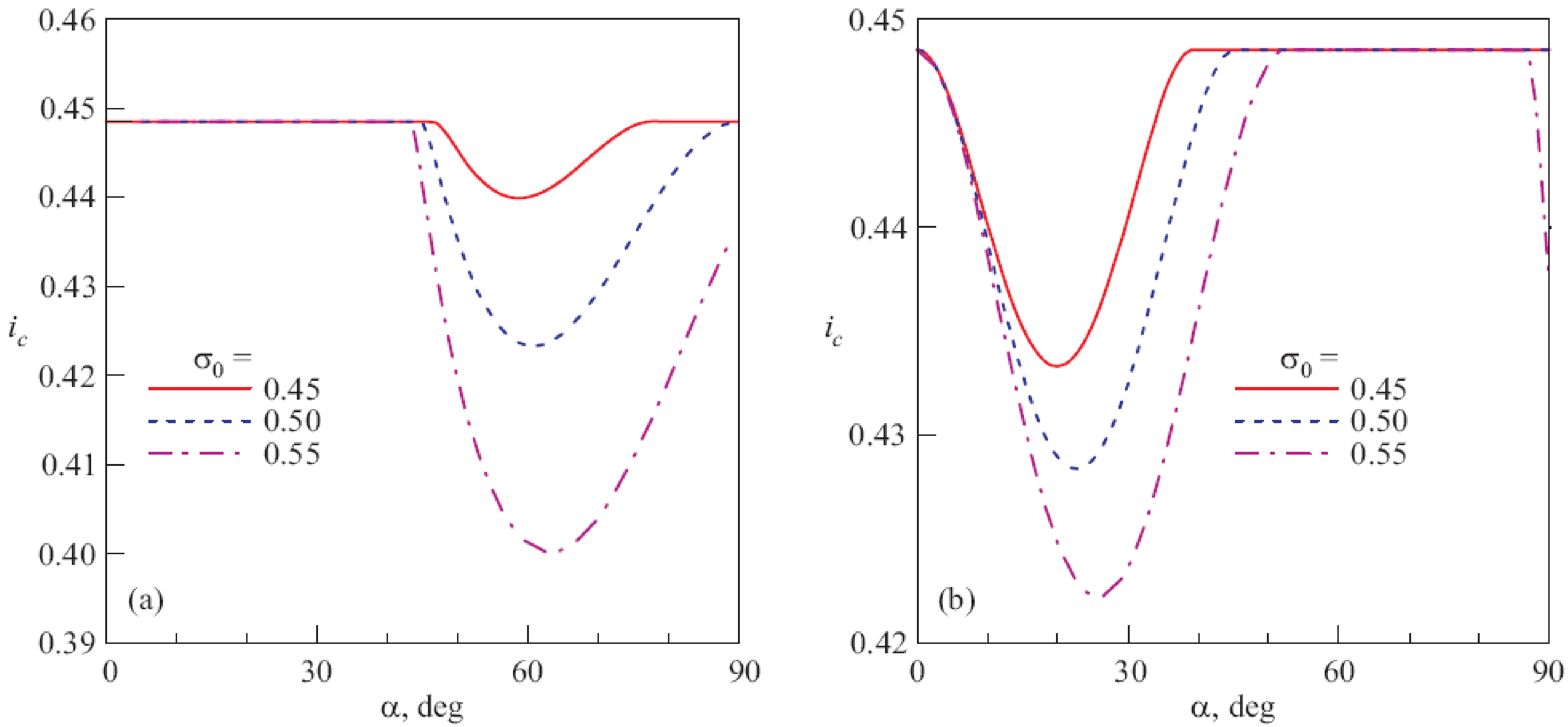

(a) $S^{d_{x^2-y^2}}_{CDW2} - I - S^{d_{x^2-y^2}}_{CDW2}$ and (b) $S^{d_{xy}}_{CDW2} - I - S^{d_{xy}}_{CDW2}$

Parameter dependences of current amplitudes in the reentrance region

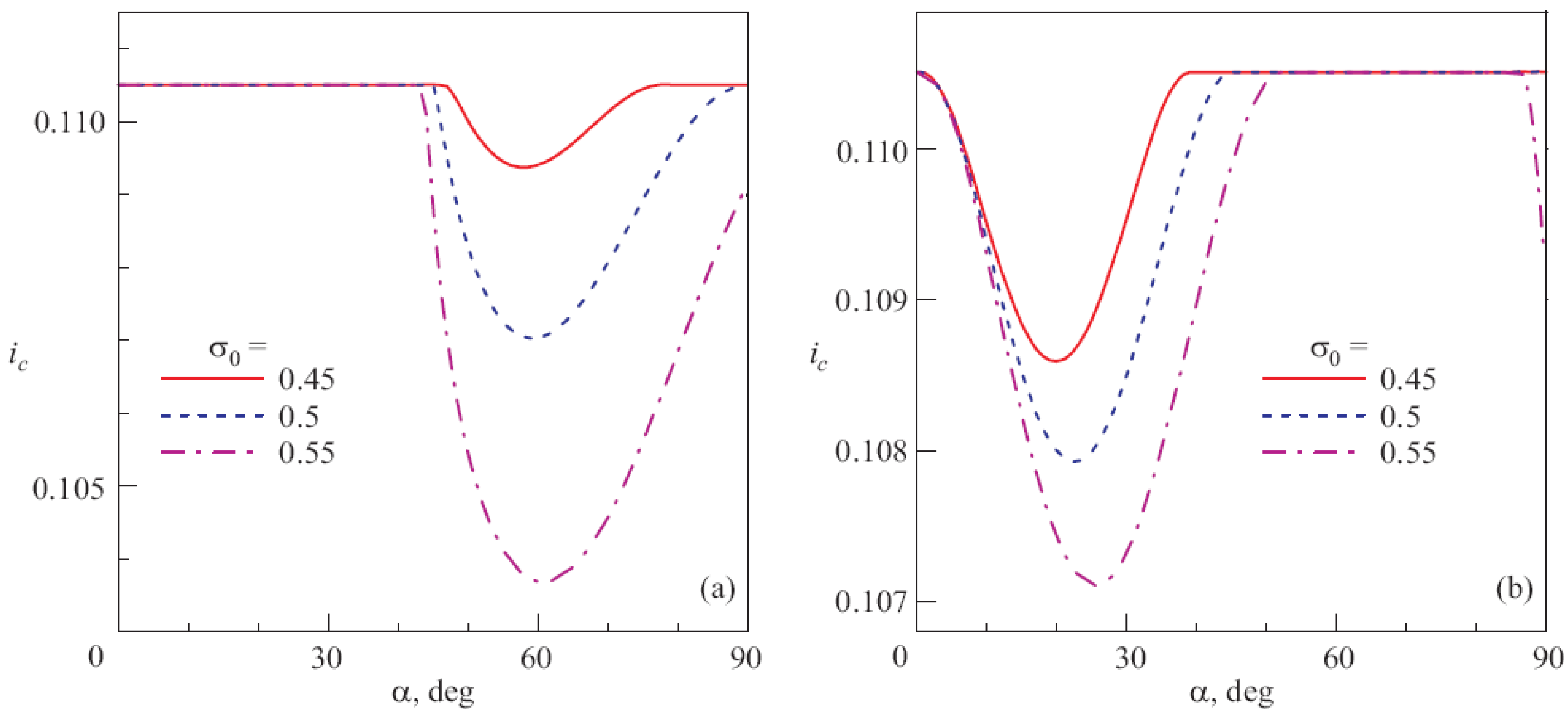

non-symmetrical $S_{CDW2}^{d_{x^2-y^2}} - I - S_{BCS}^{s}$ (a) and $S_{CDW2}^{d_{xy}} - I - S_{BCS}^{s}$ (b) junctions.

Influence on the directional tunneling angle θ_0

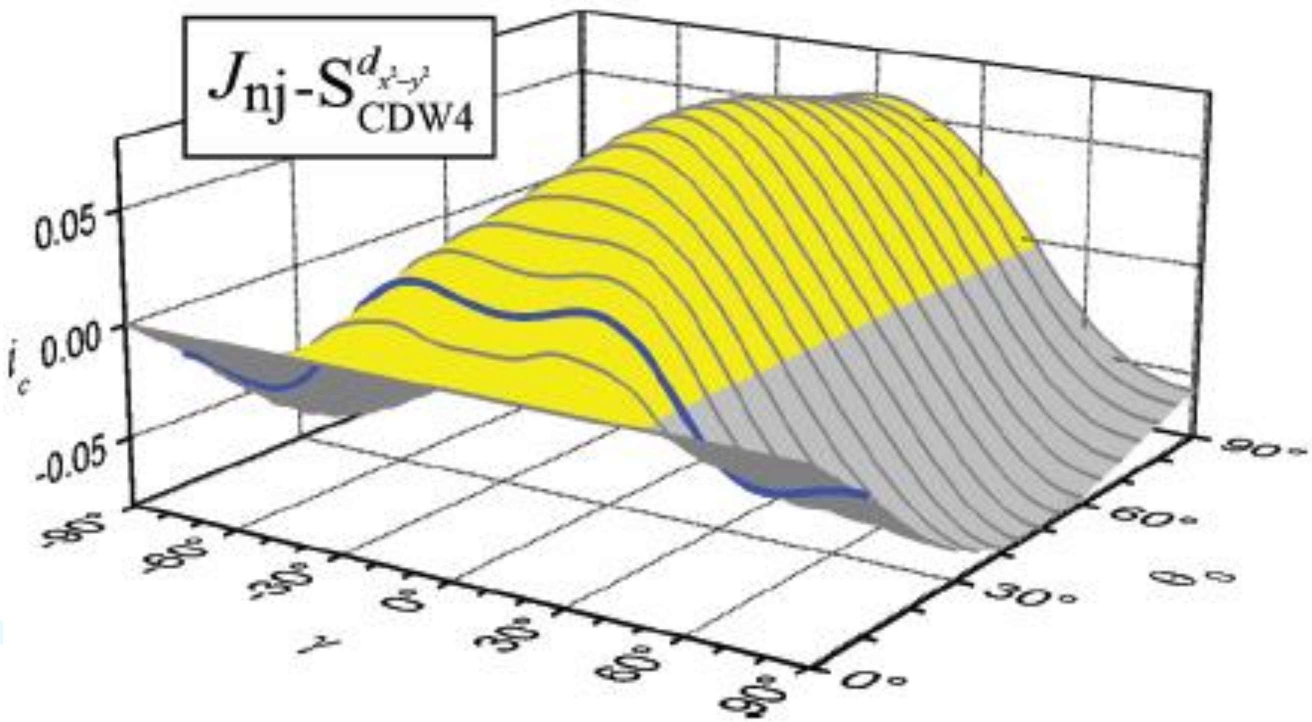

Angular current dependences for symmetric d-wave superconducting junctions with unidirectional CDWs

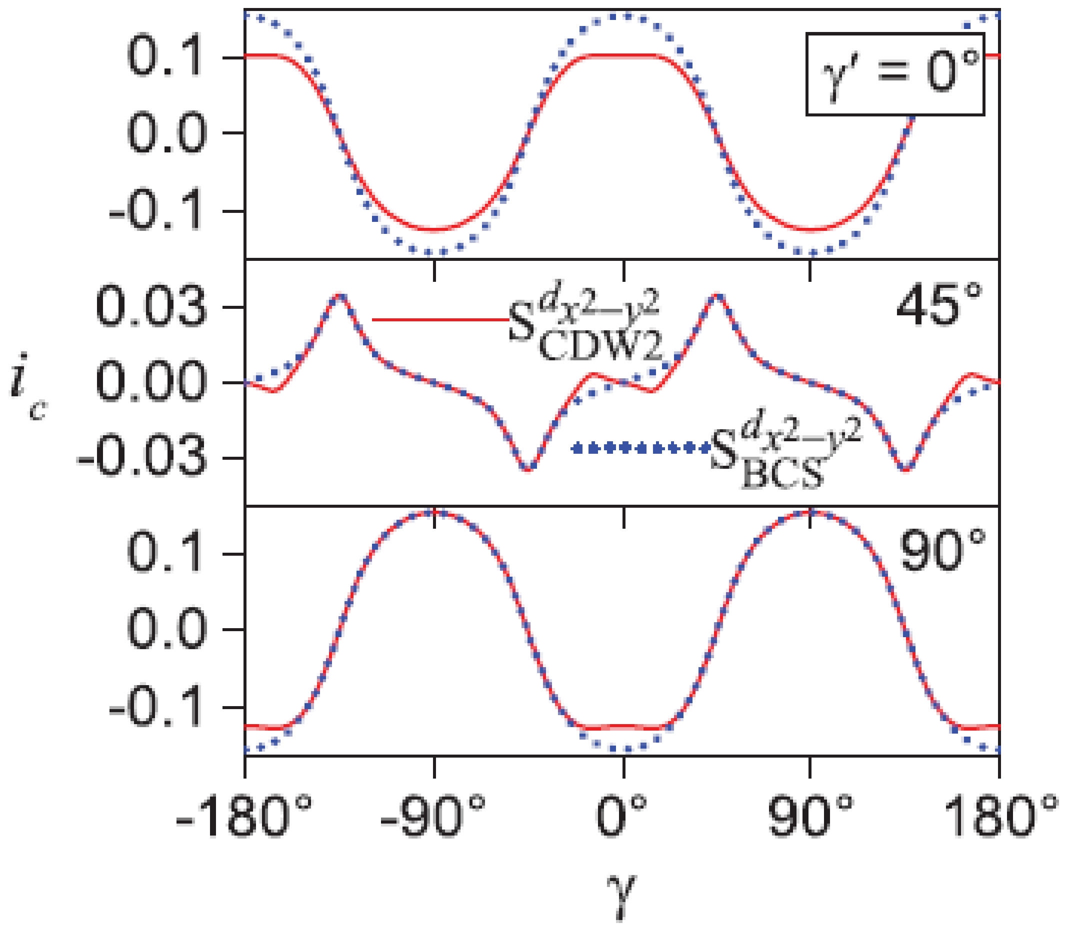

Angular current dependences for symmetric d-wave superconducting junctions with correlated rotations of checkerboard (a) and unidirectional (b) CDWs

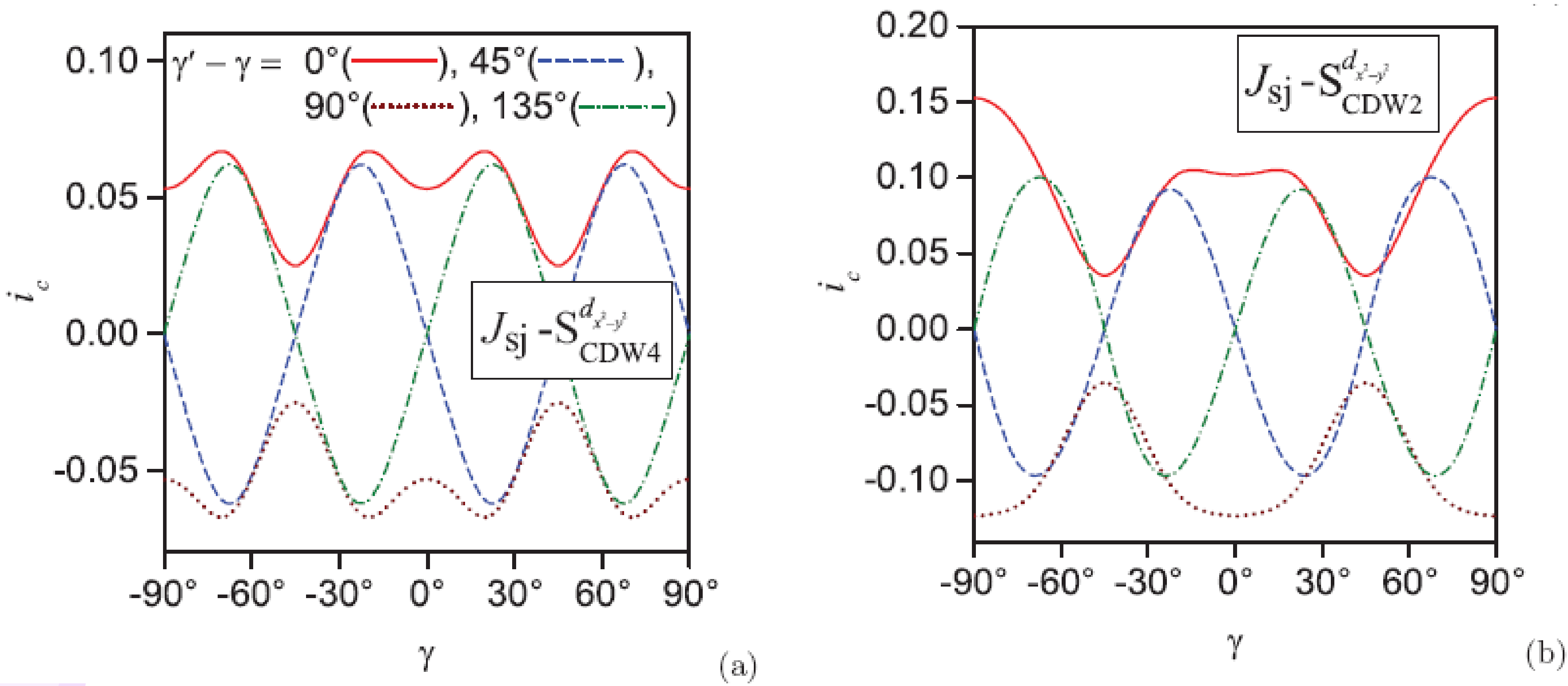

Angular current dependences for symmetric CDW superconducting junctions with different symmetries of the superconducting order parameter and checkerboard CDW configuration

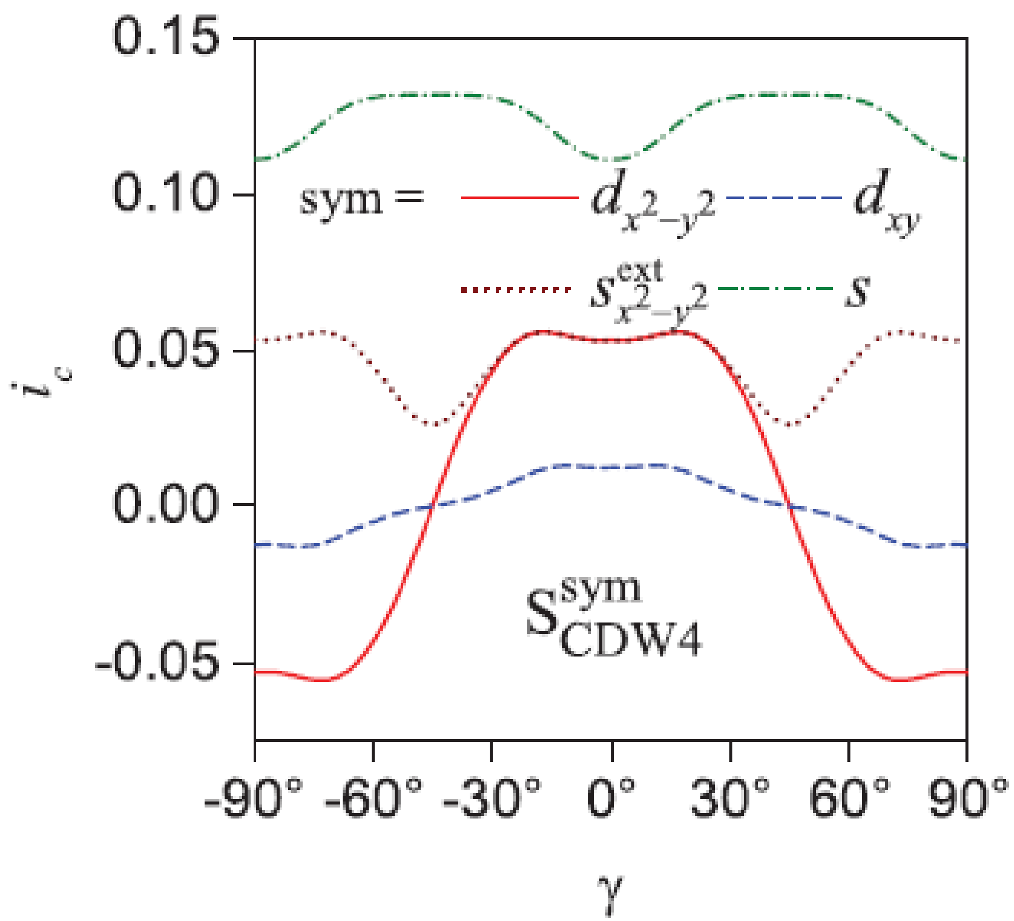

Angular current dependences for non-symmetric CDW superconducting junctions with different symmetries of the superconducting order parameter and checkerboard (a) and unidirectional (b) CDW configurations

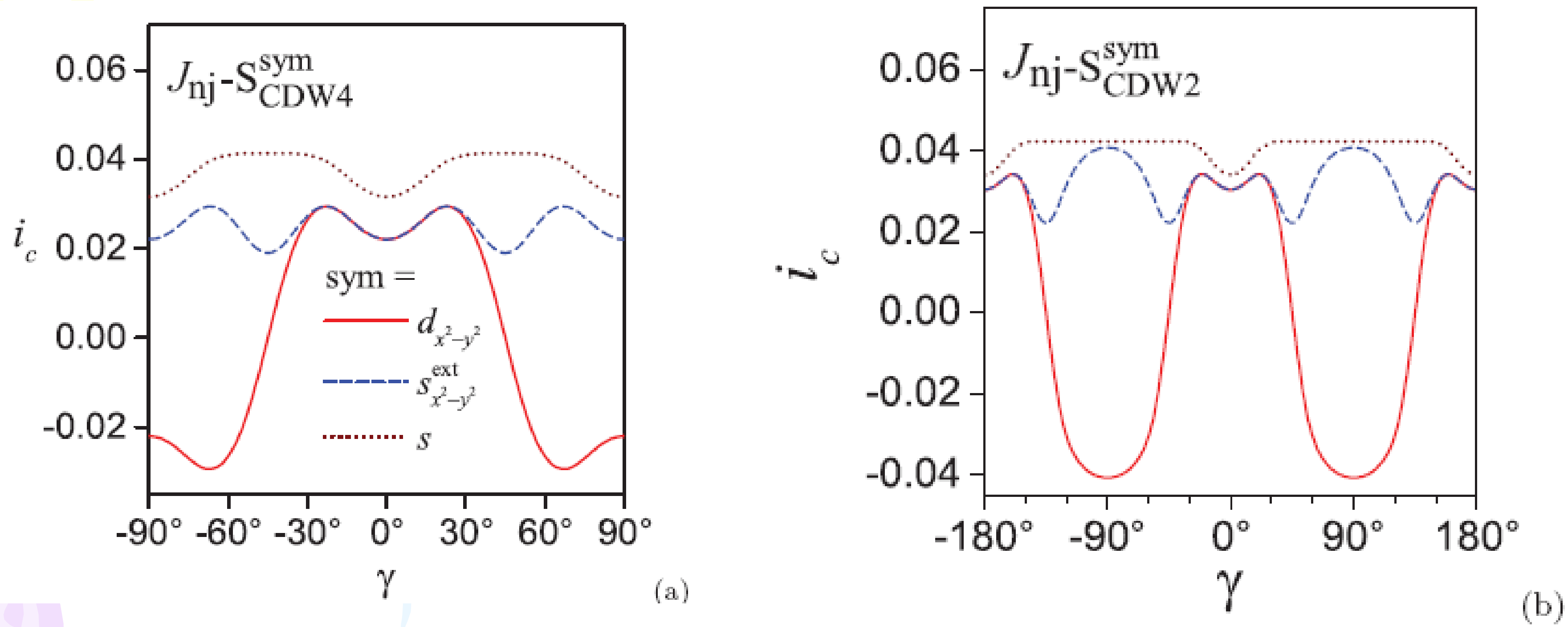

Proportionality between Josephson current and product of superconducting gaps: symmetric junctions involving d- and s-wave superconductors ($\tau = T/T_c$ as a driving force)

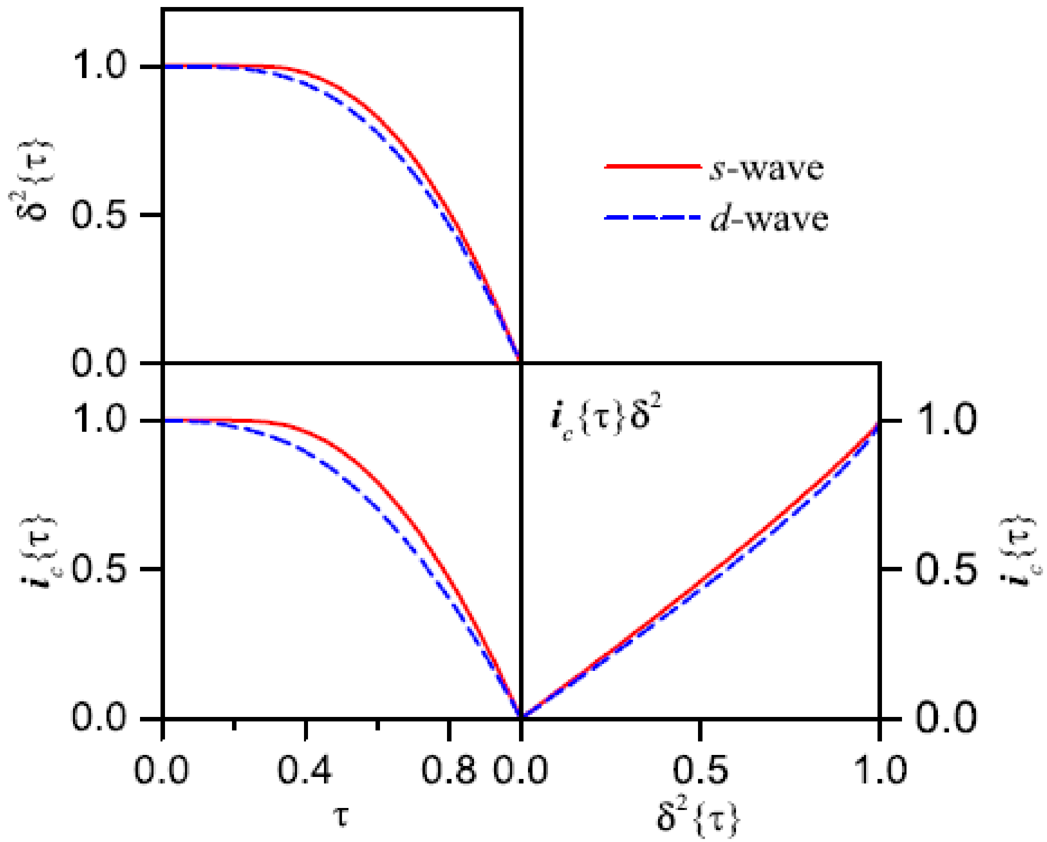

Proportionality between Josephson current and product of superconducting gaps: symmetric junctions involving d-wave superconductors with unidirectional CDWs (α as a driving force)

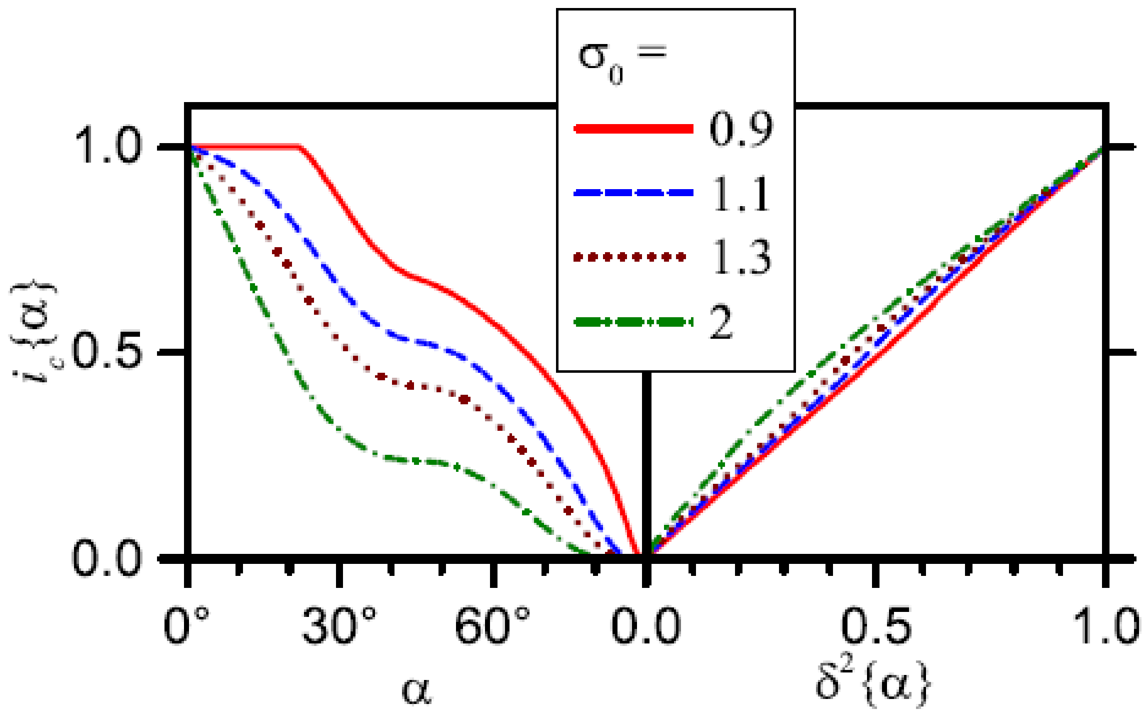

Proportionality between Josephson current and product of superconducting gaps: non-symmetric junctions involving d-wave superconductors with unidirectional CDWs (α as a driving force)

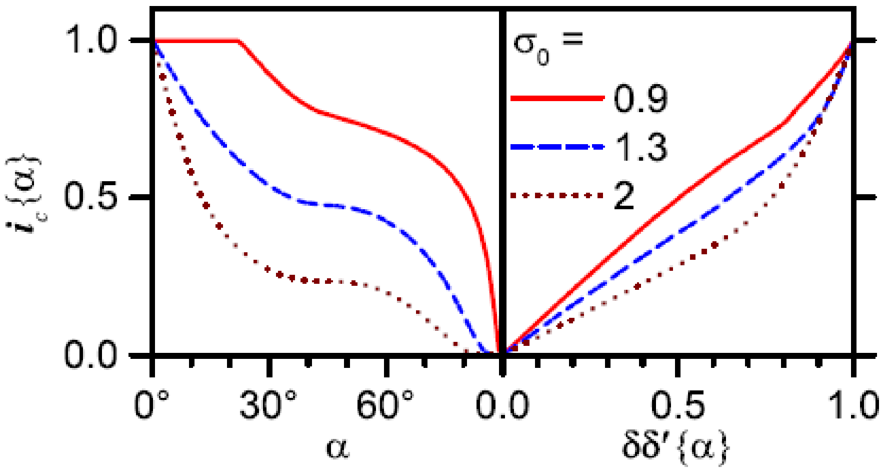

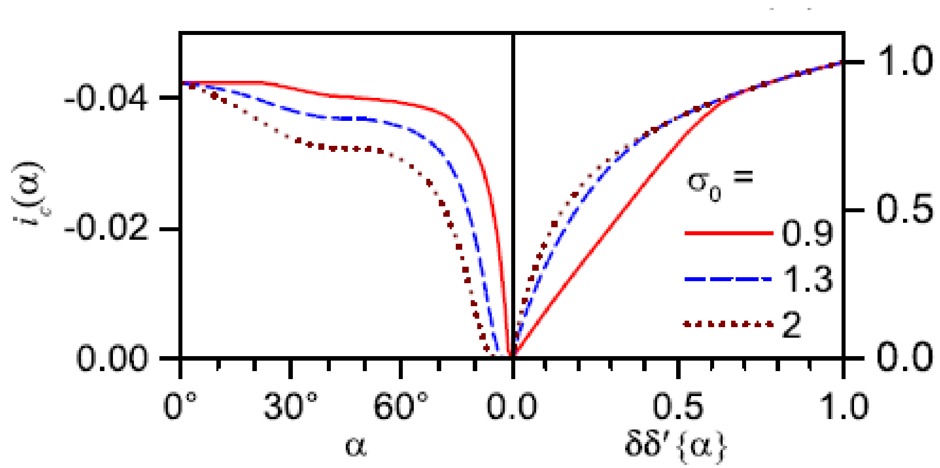

γ = 0°

γ = 90°

Temperature dependences of the Josephson current in the reentrance region and even outside this region (!) differs from the Ambegaokar-Baratoff conventional curve, $\gamma = 0$, $\gamma' = 0$ .Varying σ_0

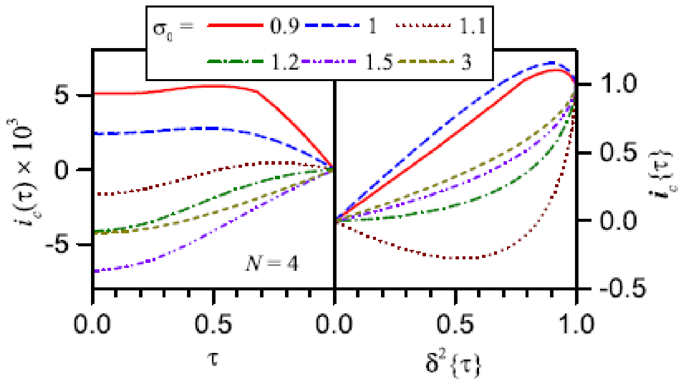

(a)

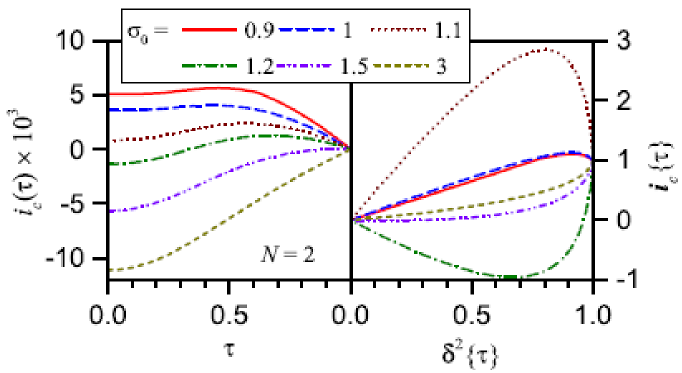

(b)

(Left panels) The normalized $i_c(\tau)$ dependences for sJ^d_{CDW2} junctions at $\alpha = 15°$ and various σ_0's for $N = 4$ (a) and 2 (b). $\gamma = 15°$, $\gamma' = 45°$, $\theta_0 = 10°$. (Right panels) The corresponding correlations $i_c\{\tau\}\delta^2$.

Proportionality between Josephson current and gap product is totally absent

Temperature dependences of the Josephson current in the reentrance region and even outside this region (!) differs from the Ambegaokar-Baratoff conventional curve , $\gamma = 0$, $\gamma' = 0$. Varying α

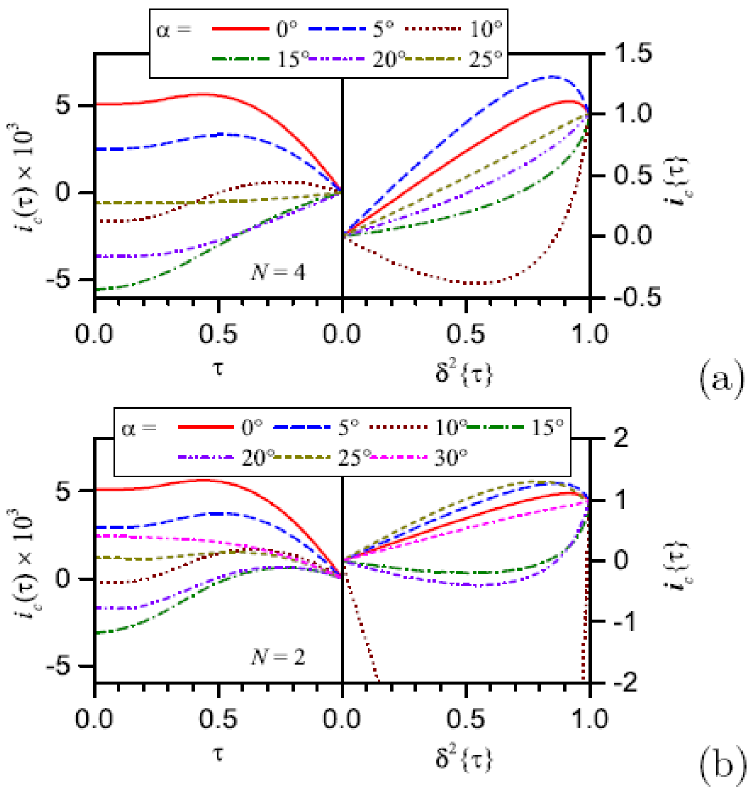

The same character of the dependences as in the previous slide

Conclusions as for Josephson tunneling

- 1. CDWs can conspicuously alter angular dependences of the stationary Josephson currents.
- 2. Angular and doping current dependences are essentially different for various possible superconducting order parameter symmetries
- 3. Angular and doping current dependences are essentially different for checkerboard and unidirectional CDWs
- 4. CDWs violate proportionality between parameter-dependent Josephson current and product of left-hand-side and right-hand-side superconducting gaps
- 5. CDWs modify temperature dependence of the stationary Josephson current so that it is no longer an Ambegaokar-Baratoff one. In ceratin T-ranges $I_c(T)$ may become non-monotonic
- 6. Josephson current measurements can supplement photoemission and tunnel spectroscopic studies to elucidate superconducting order parameter symmetry, detect CDWs and find their configuration